Published in final edited form as:
*J Cell Physiol*. 2009 April ; 219(1): 143–151. doi:10.1002/jcp.21661.

# Endogenous FGF-2 is critically important in PTH anabolic effects on bone

**Maria Giovanna Sabbieti**[1], **Dimitrios Agas**[1], **Liping Xiao**[2], **Luigi Marchetti**[1], **J. Douglas Coffin**[3], **Thomas Doetschman**[4], and **Marja M. Hurley**[2,*]

[1]Department of Comparative Morphology and Biochemistry, University of Camerino, Camerino (MC) Italy

[2]Department of Medicine, University of Connecticut Health Center, Farmington, Connecticut, USA

[3]Department of Biomedical and Pharmaceutical Sciences, University of Montana, Missoula, MT, USA

[4]BI05 Institute, University of Arizona, Tucson, AZ, USA

## Abstract

Parathyroid hormone (PTH) increases Fibroblast growth factor receptor-1 (FGFR1) and Fibroblast growth factor-2 (FGF-2) expression in osteoblasts and the anabolic response to PTH is reduced in Fgf2−/− mice. This study examined whether candidate factors implicated in the anabolic response to PTH were modulated in Fgf2−/− osteoblasts. PTH increased Runx-2 protein expression in Fgf2+/+ but not Fgf2−/− osteoblasts. By immunocytochemistry, PTH treatment induced nuclear accumulation of Runx-2 only in Fgf2+/+ osteoblasts. PTH and FGF-2 regulate Runx-2 via activation of the cAMP response element binding proteins (CREBs). Western blot time course studies showed that PTH increased phospho-CREB within 15 min that was sustained for 24 h in Fgf2+/+ but had no effect in Fgf2−/− osteoblasts. Silencing of FGF-2 in Fgf2+/+ osteoblasts blocked the stimulatory effect of PTH on Runx-2 and CREBs phosphorylation. Studies of the effects of PTH on proteins involved in osteoblast precursor proliferation and apoptosis showed that PTH increased cyclinD1-cdk4/6 protein in Fgf2+/+ but not Fgf2−/− osteoblasts. Interestingly, PTH increased the cell cycle inhibitor p21/waf1 in Fgf2−/− osteoblasts. PTH increased Bcl-2/Bax protein ratio in Fgf2+/+ but not Fgf2−/− osteoblasts. In addition PTH increased cell viability in Fgf2+/+ but not Fgf2−/− osteoblasts. These data suggest that endogenous FGF-2 is important in PTH effects on osteoblast proliferation, differentiation and apoptosis. Reduced expression of these factors may contribute to the reduced anabolic response to PTH in the Fgf2−/− mice. Our results strongly indicate that the anabolic PTH effect is dependent in part on FGF-2 expression.

### Keywords

FGF-2; PTH; Runx-2; Bcl-2; CREBs

## INTRODUCTION

Endogenous human parathyroid hormone (PTH) is an 84 amino acid peptide (PTH 1–84) that together with active fragments such as PTH 1–34 exerts contrasting effects on bone, depending upon the length of exposure. The ‘anabolic’ or bone-building effects require brief

*Corresponding author: Marja M. Hurley, Division of Endocrinology and Metabolism, University of Connecticut School of Medicine, 263 Farmington avenue, Farmington Connecticut, 06030-1850 USA, Tel. 860-6792129; Fax 860-679-1258; Hurley@exchange.uchc.edu.

exposures to PTH (Rosen et al., 2001). The 'catabolic' effects result from pathological conditions in which one or more parathyroid glands secrete too much hormone continuously at a sustained level. Such continuous secretion of PTH (as occurs in chronic renal disease and primary hyperparathyroidism) can lead to bone destruction. The principal target organs for PTH are the kidney (increasing proximal tubular resorption of calcium, phosphate excretion and 1,25 dihydroxy vitamin D formation) and the skeleton. An indirect effect, increasing intestinal calcium absorption, is mediated by the increase in 1,25 dihydroxy vitamin D3 formation in the kidney. Intermittent PTH administration results in a rapid increase in biochemical markers of bone formation, with a lesser and delayed increase in resorption markers (Hodsman et al., 2003); the same response was seen following treatment with teriparatide (Hodsman et al., 1993). When PTH is administered by a daily subcutaneous injection, an increase in bone mass occurs in both animals and humans (Hock et al., 1988; Lane et al., 1995; Neer et al., 2001; Dempster et al., 2001). In humans, the anabolic effect of PTH is most pronounced in the trabecular bone.

Basic fibroblast growth factor (FGF-2) is a potent stimulator of osteoblast precursor proliferation and is anabolic in experimental animals (Gospodarowicz, 1990; Hurley et al., 2002). It is synthesized in osteoblasts and stored in the extracellular matrix (ECM) (Hurley et al., 2002). *In vitro* studies have shown that continuous treatment with FGF-2 stimulated bone cell replication (Globus et al., 1988) and reduced differentiation related markers such as alkaline phosphatase (Shen et al., 1989) and PTH responsive adenylate cyclase activity (Rodan et al., 1989). FGF-2 signals via high affinity tyrosine kinase FGF receptors (FGFRs) that are involved in many biological processes during embryo development and homeostasis of body tissues (Hurley et al., 2002). Disruption of normal FGF receptor functions lead to pathological conditions in humans (Hurley et al., 2002; Groth and Lardelli 2002). In addition, disruption of the Fgf2 gene in mice resulted in decreased smooth muscle contractility, low blood pressure and thrombocytosis (Zhou et al., 1998). Furthermore, Fgf2−/− mice showed significantly decreased bone mass and bone formation (Montero et al., 2000).

Similar to FGF-2, PTH increases bone formation *in vivo* (Hock et al., 1989), decreases bone formation *in vitro* (Kream et al., 1993), and maintains serum calcium concentration by stimulating bone resorption (Reeve, 1996). In MC3T3-E1 osteoblasts, PTH increases FGF-2 gene expression and also regulates FGF receptor expression (Hurley et al., 1999). Moreover, endogenous FGF-2 may be important in PTH-induced osteoclast formation since in vitro studies showed impaired osteoclast formation and impaired hypercalcemic response to high dose acute PTH in vivo in Fgf2−/− mice (Okada et al., 2003). In addition, the bone anabolic response to PTH is markedly impaired in Fgf2−/− mice (Hurley et al., 2006). Furthermore, we previously reported that the increase in bone anabolic markers in PTH-treated patients with glucocorticoid-induced osteoporosis was associated with increased levels of serum FGF-2 (Hurley et al., 2005). It is also important to note that many of the signal molecules, involved in osteoblast survival and differentiation that are regulated by PTH, are also modulated by FGF-2 (Hurley et al., 2002). Hence, these similarities raised the intriguing possibility that some effects of PTH on bone cell functions may be modulated by endogenous FGF-2 production.

Although *in vivo* studies have established an essential role for FGF-2 and PTH in bone formation, the mechanism of FGF-2 and PTH action in osteoblasts is not well understood and appears to be complex, involving multiple signalling pathways and factors. Both PTH and FGF-2 prolong osteoblast lifespan by increasing the survival gene Bcl-2 and decreasing the pro-apoptotic gene Bax (Jilka et al., 1999; Mansukani et al., 2000). It was also demonstrated that Runx-2 (Pebp2αA) is essential for the differentiation of osteoblasts from mesenchymal precursors (Otto et al., 1997) and the protein kinase A (PKA) pathway

activated by PTH may also stimulate phosphorylation of Runx-2 (Franceschi et al., 2003). Moreover, it was shown that FGF-2 phosphorylates and activates Runx-2 via activation of MAPK pathway (Xiao et al., 2002). In addition the cAMP response element binding proteins (CREBs) that regulates cellular proliferation, differentiation, adaptation and survival is modulated by PTH (Long et al., 2001) as well as FGF-2 (Tane t al., 1996).

The goal of this study was to examine the role of endogenous FGF-2 in the modulation of signalling molecules implicated in the bone anabolic response of PTH using the Fgf2−/− mouse model.

## MATERIALS AND METHODS

### Animals

Fgf2 null mice were developed as previously described (Zhou et al., 1998). Mice were bred and housed in the transgenic facility in the Center for laboratory animal care at the University of Connecticut Health Center. Mice were sacrificed by $CO_2$ narcosis and cervical dislocation. The Animal Care and Use Committee of the University of Connecticut Health Center approved animal protocols.

### Primary calvarial osteoblast cells (COBs)

Cells were digested from calvariae of newborn Fgf2+/+ and Fgf2−/− mice in a solution of 1 ml trypsin as previously described (Montero et al., 2000). Cells were pooled and then cultured to confluence in 100-mm dishes. Then, they were resuspended and replated in 6-well dishes at 5000 cells/$cm^2$, and cultured in α-MEM (Invitrogen Life Technologies, Grand Island, New York, USA) containing 10% heat inactivated fetal calf serum (HFCS), penicillin (100 U/ml) and streptomycin (50μg/ml).

### Western Blotting

Fgf2+/+ and Fgf2−/− primary COBs were plated at $10\times10^6$ cells/well in 6 well culture dishes and grown in appropriate medium with 10% HFCS, penicillin and streptomycin, until confluence. Cells were serum deprived for 24 h and stimulated with PTH (from $10^{-8}$ M to $10^{-10}$ M; Sigma Aldrich) from 15 min to 24 h. Control cultures were treated with appropriate vehicle. Proteins were extracted with Cell Lysis buffer (Cell Signaling) and the concentration was determined by the BCA protein assay reagent (Pierce, Celbio, Italy). After SDS-polyacrylamide gel electrophoresis on 12% gels, proteins were transferred to PVDF membranes (Amersham Biosciences, Europe, GMBH). The next steps were performed by ECL Advance Western Blotting Detection Kit (Amersham Biosciences). Briefly, membranes were blocked with Advance Blocking Agent in PBS-T (PBS containing 0.1% Tween 20) for 1 h at room temperature. Then, membranes were incubated for 2 h at room temperature with the following primary antibodies: rabbit anti-Pebp2aA (Runx-2) antibody (Santa Cruz Biotechnology, Santa Cruz, CA); rabbit anti-phospho-CREBs antibody (Upstate Biotechnology); rabbit anti-phospho-p44/42 MAP Kinase antibody (Cell Signaling Technology, Beverly, MA); rabbit anti-cyclin D1 antibody (Cell Signaling Technology, Beverly, MA); rabbit anti-cdk4 antibody (Cell Signaling Technology, Beverly, MA); rabbit anti-cdk6 antibody (Cell Signaling Technology, Beverly, MA); rabbit anti- Bcl-2 antibody (Santa Cruz Biotechnology, Santa Cruz, CA); rabbit anti-Bax antibody (Santa Cruz Biotechnology, Santa Cruz, CA). After washing with PBS-T the blots were incubated with horseradish peroxidase (HRP)-conjugated donkey anti-rabbit IgG (Amersham Biosciences) diluted 1:100,000 in blocking solution for 1 h at room temperature. After further washing with PBS-T, immunoreactive bands were visualized using luminol reagents and Hyperfilm-ECL film (Amersham Biosciences) accordingly to the manufacturer's instructions. To normalize the bands, filters were stripped and re-probed with a rabbit anti-α-tubulin

antibody (Sigma Aldrich) or with a rabbit anti-p44/42 antibody. Signal was detected by KODAK MR-1 autoradiography. Band density was quantified densitometrically.

### Cell culture for immunofluorescence

Fgf2+/+ and Fgf2−/− COBs were plated at 5000 cells/cm$^2$, on coverslips previously cleaned and sterilized, and grown for 4 days in medium containing 10% HFCS, penicillin and streptomycin. When at least 80% of confluence was reached, cells were serum deprived for 24 h and treated with PTH ($10^{-9}$ M) or FGF-2 ($10^{-9}$ M). Cells were fixed in 4% paraformaldehyde in PBS for 20 min at room temperature and permeabilized with 0.3% Triton X-100 in PBS for 30 min. Cells were washed in PBS and incubated with 0.5% BSA dissolved in PBS at room temperature for 20 min. Then, cultures were incubated, for 2 h at room temperature, with the following primary antibodies: rabbit anti-Pebp2aA (Santa Cruz Biotechnology, Santa Cruz, CA) diluted 1:30 in PBS; rabbit anti-phospho-p44/42 MAP Kinase (Cell Signalling Technology, Beverly, MA) diluted 1:50 in PBS; rabbit anti-phospho-CREBs (Upstate Biotechnology) diluted 1:50 in PBS. After washing with PBS, cells were incubated with Alexa Fluor 488 chicken anti-rabbit IgG (Molecular Probe) for 1 h at room temperature. Reaction controls were performed using a non-immune rabbit immunoglobulin IgG, by complexing the primary antibody with a relative blocking peptide or by omitting the primary antibody. Coverslips were mounted on slides with PBS/glycerol (1:1). Slides were imaged using fluorescent microscopy on Zeiss Axioplan microscopy.

### CMV/Fgf2/ires/eGFP Retroviral Vector Construction and Cell Infection

CMV/ires/eGFP (pMg1cla) vector containing the enhanced GFP (eGFP) gene driven from an internal cytomegalovirus (CMV) promoter was previously described (Dong et al., 2004). The coding sequence of the Fgf2 was cloned into the EcoRI site of the CMV/ires/eGFP retroviral vector. eGFP was used to visualize expression of protein mediated by CMV vectors in cells. Control virus was CMV/ires/eGFP vector without inserted Fgf2 cDNA. 293GPG packaging cell lines were infected by CMV/ires/eGFP or CMV/Fgf2/ires/eGFP vector using the LipofectMINE™ 2000 Reagent (Invitrogen Life Technologies, Carlsbad, CA) following product protocol. Infected 293GPG packaging cell lines were grown in high-glucose Dulbecco's modified Eagle's medium (DMEM; Life Technologies, Rockville, MD) containing 10% heat-inactivated fetal bovine serum (HIFBS), 1mg/ml of puromycin, 1mg/ml of tetracycline and 0.4mg/ml of G418. To produce vector virus, tetracycline and G418 were removed from the media, then conditioned media were collected after 24, 48, 72, and 96 h, filtered through a 0.2 mm Nalgene filter. Condition media was measured for reverse transcript activity by measurement of virus production and then frozen at −80°C.

### Transduction of Mouse Primary Calvarial Osteoblasts

Primary calvarial osteoblasts from Fgf2−/− mice were plated in 6 well dishes and grown in α-MEM (Sigma-Aldrich) containing 10% HIFCS plus 100U/ml of penicillin and 100mg/ml of streptomycin. Cells were transduced with virus when 50% confluent. Media including 5 mL of virus-containing media, 5 mL of α-MEM containing 10% HFCS and 8 mg/mL of protamine sulfate was added to the cell cultures for approximately 16 h, followed by fresh media replacement during 8 h. The cells were exposed to three cycles of virus infection. Expression of eGFP was examined by a Zeiss Axioplan fluorescent microscopy.

### RNA interference (siRNA)

To specifically study the role of FGF-2 in PTH modulation of Runx-2 and CREBs syntheses as well as Bcl-2/Bax ratio, COBs were plated in 6-well dishes culture dishes (Costar Corp.) at a density of $10\times10^6$ cells/well and grown for 5 days in a-MEM (Invitrogen Life Technologies, Grand Island, New York, USA) containing 10% HFCS, penicillin (100 U/ml)

and streptomycin (50 μg/ml). Other cultures were transfected with FGF-2 siRNA according to siRNA transfection protocol from the manufacture (Santa Cruz Biotechnology, Inc., Italy). A control siRNA (non-homologous to any known gene sequence) was used as a negative control. The levels of FGF-2 were analyzed by Western blotting using a rabbit anti-human FGF-basic antibody (PeproTec EC Ltd, Inalco SPA, Italy) and the specificity of the silencing was confirmed in three different experiments. COBs transfected with control siRNA and with FGF-2 siRNA were 24 h serum deprived before addition of PTH ($10^{-9}$ M) or vehicle for 24 h. Proteins were extracted and processed as described above; filters were incubated for 2 h at room temperature with the following primary rabbit anti-Runx-2 antibody (Santa Cruz Biotechnology, Inc., Italy), with rabbit anti-phospho-CREBs antibody (Upstate Biotechnology), rabbit anti-Bcl-2 antibody (Santa Cruz Biotechnology, Santa Cruz, CA) and rabbit anti-Bax antibody (Santa Cruz Biotechnology, Santa Cruz, CA). The next steps were performed as described above. To normalize the bands, filters were stripped and re-probed with a monoclonal anti-α-tubulin (Sigma-Aldrich, Milano, Italy). Bands density was quantified densitometrically.

### Assessment of the metabolic activity of viable COBs (MTS)

The metabolic activity of viable cells was determined by the MTS [3-(4,5-dimethylthiazol-2-yl)-5-(3-carboxymethoxyphenyl)-2-(4-sulfophenyl)-2H-tetrazolium] assay. Briefly, COBs were plated at the density of 5,000 cells/well in 96 culture dishes (Costar Corp., Celbio, Italy) and grown in α-MEM (Invitrogen Life Technologies, Grand Island, New York, USA), supplemented with 10% heat inactivated fetal calf serum (FCS, Invitrogen, Italy), penicillin and streptomycin to approximately 80% confluence. Cells were serum deprived for 24 h and treated with PTH (from $10^{-9}$ M to $10^{-11}$ M) or FGF-2 ($10^{-9}$ M) for an additional 24 h. Other cells were treated with only vehicle. Then, cells were incubated with 20 μl/well of CellTiter 96 $AQ_{ueous}$ One Solution Reagent (Promega Italia srl, Milano, Italy) and incubated for 2 h in a humidified, 5% $CO_2$ atmosphere. The quantity of formazan product is directly proportional to the number of living cells in culture. The colored formazan was measured by reading the absorbance at 490 nm using a 96 well plate reader.

## RESULTS

### Effect of PTH on Runx-2 protein in COBs from Fgf2+/+ and Fgf2−/− mice

In order to investigate the involvement of FGF-2 in PTH regulation of Runx-2 protein levels, COBs from Fgf2+/+ and Fgf2−/− mice were treated with PTH (from $10^{-8}$ M to $10^{-10}$ M) for 24 h. Dose response and time course studies showed that PTH $10^{-9}$ M caused a maximal increase in Runx-2 at 24 h only in COBs from Fgf2+/+ mice (Fig. 1A,B). Pooled data from four independent experiments showed that 24 h of PTH treatment increased Runx-2 protein by 65% in Fgf2+/+ COBs with no effect on COBs from Fgf2−/− mice (Fig. 1C). Since Runx-2 acts inside the nucleus, immunocytochemical experiments were performed to study protein localization in COBs after PTH treatment. Figure 1D shows that PTH induced an increase of Runx-2 particularly evident into the perinuclear and nuclear area in COBs from Fgf2+/+ mice but not from Fgf2−/−mice. The response to PTH in Fgf2+/+ cells, was consistent with that observed with FGF-2 ($10^{-9}$ M) in Fgf2−/− cells indicating the importance of FGF-2 on Runx-2 nuclear accumulation.

### Effect of PTH on phospho-ERK in COBs from Fgf2+/+ and Fgf2−/− mice

Since previous studies reported that the MAPK pathway was important in FGF-2 regulation of Runx-2 expression in osteoblasts, time course experiments were performed to study the effect of PTH on phospho-p44/42 in osteoblasts from Fgf2+/+ and Fgf2−/− mice. Western blotting showed that treatment with PTH for 6 h and 24 h strongly increased phospho-

p44/42 ERK proteins in Fgf2+/+ COBs. In contrast, PTH decreased phospho-p44/42 at 6 and 24 h in Fgf2−/− COBs (Fig. 2A). Pooled data from three independent experiments showed a statistically significant increment of phospho-p44/42 proteins after 6 h and 24 h of PTH treatment, only in Fgf2+/+ COBs (Fig. 2B).

### Effect of PTH on phospho-CREBs

We also assessed whether loss of Fgf2 gene would alter phospho-CREBs by PTH. COBs from both genotypes were treated from 15 min to 24 h with vehicle or PTH and Western blots showed that PTH strongly increased phospho-CREBs in Fgf2+/+ cultures within 15 min that was sustained for 24 h. In contrast, PTH was unable to increase phospho-CREBs in Fgf2−/− cultures (Fig. 3A). Immunocytochemistry showed that at 24 h both PTH and FGF-2 increased the cytoplasmic labeling of phospho-CREBs in Fgf2+/+ cultures. In contrast to FGF-2, PTH did not increase phospho-CREBs in Fgf2−/− cultures (Fig. 3B).

### Effect of PTH on Runx-2 and phospho-CREBs in FGF-2 silenced Fgf2+/+ COBs

To verify the role of FGF-2 in Runx-2 and CREBs modulation by PTH, an RNAi approach was used to deplete FGF-2. siRNA efficiently and specifically silenced (more than 80%) FGF-2 expression in COBs (Fig. 4A). In particular, in control siRNA transfected COBs, treatment with PTH ($10^{-9}$ M) increased Runx-2 and CREBs, as above observed in non-transfected osteoblasts. Interestingly, the depletion of FGF-2 by the specific siRNA, blocked the increased synthesis of both Runx-2 and CREBs induced by PTH ($10^{-9}$ M) (Fig. 4B). Pooled data of three independent experiments confirming the above results is shown in Fig. 4C.

### Effect of PTH on Runx-2 and CREB accumulation and nuclear localization in Fgf2−/− COBs transfected with the Fgf2 construct

To further analyze the above data, Fgf2−/− COBs were transfected with a vector or FGF-2 retrovirus. *In situ* experiments showed GFP labeling in cells transfected with the vector (Figs. 5Aa, Ba) or Fgf2 coding sequence (Figs. 5Ac, Bc). PTH did not increase Runx-2 in cells transfected with the vector construct (Fig. 5Ab) but increased Runx-2 nuclear labeling in Fgf2−/− cells transfected with the FGF-2 coding sequence (Fig. 5Ad). Similarly, PTH did not increase phospho-CREBs labeling in Fgf2−/− cells transfected with the vector construct (Fig. 5Bb) but marked nuclear labeling was observed in Fgf2−/− cells transfected with the Fgf2 coding sequence (Fig. 5Bd). FGF-2 treatment increased Runx-2 protein and phospho-CREBs in cells transfected with either vector or Fgf2 coding sequence (Figs. 5Ab, Ad; 5Bb, Bd).

### Effect of PTH on cyclin D1 and cdk4/6 in COBs from Fgf2+/+ and Fgf2−/− mice

Numerous studies have shown that differentiation requires exit from cell cycle (Jilka, 2007) and PTH was previously shown to decrease expression of cyclin D1 in osteoblast cultured in differentiation media (Datta et al., 2005). We therefore examined the effects of PTH on cyclin D1, cdk4/6 in COBs from both genotypes, then serum deprived for 24 h prior to treatment with vehicle or PTH ($10^{-9}$ M) for 4 to 24 h. Western blotting experiments indicated that PTH increased cyclin D1 and cdk4/6 only in COBs from Fgf2+/+ mice (Fig. 6A). Consistently, increased synthesis of p21 was found only in Fgf2−/− COBs (Fig. 6B).

### Effect of PTH on Bcl-2/Bax ratio in COBs from Fgf2+/+ and Fgf2−/− mice

Studies have shown that PTH, by increasing cell survival, contributes to an increased osteoblasts number (Jilka, 2007). Therefore, the importance of FGF-2 in PTH regulated osteoblasts survival was studied in Fgf2+/+ and Fgf2−/− COBs. Time course studies show that PTH ($10^{-9}$ M) caused a maximal increase in Bcl-2/Bax ratio only in Fgf2+/+ COBs at

24 h (Fig. 7 A). The results were, also, confirmed by silencing FGF-2 as shown in Fig. 7B. Since an increase of Bcl-2/Bax ratio suggests an increment of cell survival, an MTS assay was performed. Treatment with PTH (from $10^{-9}$ M to $10^{-11}$ M) for 24 h caused an increase cell viability that was dose dependent with a maximal increase at $10^{-9}$ M only in Fgf2+/+ COBs (Fig. 7C). The response to PTH in Fgf2+/+ COBs was similar to that observed with FGF-2 $10^{-9}$ M in Fgf2−/− COBs (Fig. 7C).

## DISCUSSION

It was previously reported that FGF-2 influences osteoblast differentiation from an early stage through a regulatory circuit mediated by the transcriptional actions of Cbfa1/Runx-2 (Choi et al., 2005). It was also demonstrated that Cbfa1/Runx-2 play a pivotal role in mediating the anabolic effects of PTH on bone through activation of the PKA pathway (Krishnan et al., 2003). Runx-2 is a bone-related transcription factor essential for the differentiation of osteoblast from mesenchymal precursors and bone formation; in fact, homozygous *Cbfa1*$^{-/-}$ mice show a complete lack of functional osteoblasts and are devoid of mineralized bone or hypertrophic cartilage (Otto et al., 1997; Komori et al., 1997). Moreover, Cbfa1 directly regulates the expression of osteocalcin, osteopontin and bone siaoloprotein, since the expression of these three genes is abolished in the cbfa1 null mice (Ducy, 2000; Ducy et al., 1997). It should be noted that osteocalcin and bone sialoprotein gene expression were both reduced in osteoblasts from Fgf2−/− mice (Naganawa et al., 2007). In the present study, Western blot analysis and immunolabeling approaches demonstrated an increased amount and nuclear accumulation of Runx-2 only in Fgf2+/+ osteoblasts stimulated for 24 h with PTH. Interestingly, the Runx-2 expression in Fgf2 knockout vehicle treated cells is higher than in Fgf2 wild type vehicle treated cells. These findings could be due to the fact that in absence of FGF-2, G1/S transition is delayed with consequent increased expression of RUNX-2 protein as previously demonstrated by Galindo et al., 2005. However, its to be emphasized that treatment with PTH increase RUNX-2 protein synthesis and perinuclear and nuclear accumulation only in Fgf2 wild type osteoblasts.

These results, thus, implicate a functional requirement for FGF-2 expression in the bone anabolic activity induced by PTH.

It was also shown that the activation of cAMP/PKA and PKC pathway by PTH could regulate other transcription factors such as CREBs (Karaplis and Goltzman, 2000). CREBs phosphorylation is a critical intermediate in endochondral bone formation (Long et al., 2001). Of interest, are the studies by Tan et al, (1996) who demonstrated that FGF-2 increased CREBs phosphorylation at Ser133 in non-osteoblastic cells. In this regard, we analyzed the modulation of phospho-CREBs in PTH treated Fgf2+/+ and Fgf2−/− osteoblasts and our results support an involvement of FGF-2 in PTH regulated phospho-CREBs.

To further demonstrate the above results, we first used the specific FGF-2 siRNA in osteoblasts from Fgf2+/+ mice; then we transfected osteoblasts from Fgf2−/− mice with the missing gene. Importantly, Western blotting studies demonstrated that specific knockdown of FGF-2 expression in COBs from Fgf2+/+ mice blocked the increment in both Runx-2 and CREBs induced by PTH. In parallel, immunocytochemical approaches confirmed that PTH was able to induce nuclear accumulation of Runx-2 and CREBs after FGF-2 gene transfection in Fgf2−/− COBs. Thus, we show for the first time that endogenous FGF-2 is important in PTH regulation and nuclear accumulation of significant transcription factors such as Runx-2 and CREBs that play critical roles in osteoblast differentiation. Reduced

expression of these factors may contribute to the reduced anabolic response to PTH in the Fgf2−/− mice.

Mechanistic studies have shown that the anti-mitotic effect of PTH is due to decreased expression of cyclin D1, which is required for cell cycle progression, as well as increased expression of cyclin-dependent kinase inhibitors $p27^{KIP1}$, $p21^{Cip1}$ and p16, which inhibit cell cycle progression (Qin et al., 2005). As previously reported, parathyroid hormone uses multiple mechanisms to arrest the cell cycle progression of osteoblastic cells from G1 to S phase (Qin et al., 2005). PTHrP signaling targets cyclin D1 and induces osteoblastic cell growth arrest (Swarthout et al., 2002). In line with those data the effects of PTH on cyclin D1, cdk4/6 was investigated in presence or absence of FGF-2. As shown under results, Western blotting experiments indicated that PTH increased cyclin D1 and cdk4/6 only in COBs Fgf2+/+. The increased synthesis of cyclin D1, cdk4/6 found in Fgf2+/+ COBs by PTH administration seem to discordant with previous data demonstrating reduced cyclin D1 expression in the presence of PTH (Datta et al., 2005; Qin et al., 2005). However, more recent studies show that cyclin D1 is a target for the proliferative effect of PTH and PTHrP in early osteoblastic cells (Datta et al., 2007; Pettway et al., 2007). It is postulated that these differential effects of PTH on cyclinD1 is developmentally stage specific (Datta et al., 2007).

Since it was demonstrated that PTH regulated bone metabolism by modulating Bcl-2/Bax ratio (Chen et al., 2002), we studied the synthesis of Bcl-2/Bax ratio in response to PTH in osteoblasts from Fgf2+/+ and Fgf2−/− mice. Bone apoptosis is important during embryonic limb development, skeletal maturation and modelling, adult bone turnover by remodelling and during fracturing healing and regeneration (Hock et al., 2001). Members of the Bcl-2 family, including Bcl-2 and Bax, are central regulators of apoptosis that promote (Bax) or inhibit (Bcl-2) cell death. Although the competition between Bax and Bcl-2 exists, each is able to regulate apoptosis independently (Knudson and Korsmeyer, 1997); thus, the ratio of Bcl-2/Bax is an important indicator of apoptosis. As previously noted, studies showed that the increased cell survival is the major contributor to increased osteoblasts number caused by PTH (Jilka, 2007) with subsequent increment of survival genes like Bcl-2 (Bellido et al., 2003). Moreover, FGF-2 plays an anti-apoptotic role in osteoblasts (Hurley et al., 2002; Agas et al., 2007). Therefore, the importance of FGF-2 in PTH regulated osteoblasts survival was studied in Fgf2+/+ and Fgf2−/− COBs. Our results clearly demonstrate that PTH increased Bcl-2 synthesis only in COBs from Fgf2+/+ mice. These data suggest that PTH may increase cell viability by an anti-apoptotic mechanism involving FGF-2.

In conclusion, the results of the present study strongly indicate that the anabolic PTH effect is dependent in part on FGF-2 expression.

## Acknowledgments

Contract grant sponsors: NIH grant AG021189 to M. M. Hurley, University of Camerino; PRIN 2005 Italy

## REFERENCES

Agas D, Marchetti L, Menghi G, Materazzi S, Materazzi G, Capacchietti M, Hurley MM, Sabbieti MG. Anti-apoptotic Bcl-2 enhancing requires FGF-2/FGF receptor 1 binding in mouse osteoblasts. J Cell Physiol. 2007; 241:145–152.

Bellido T, Ali AA, Plotkin LI, Fu Q, Gubrij I, Roberson PK, Weinstein RS, O'Brien CA, Manalagos SC, Jilka RL. Proteasomal degradation of Runx-2 shortens parathyroid hormone-induced anti-apoptotic signaling in osteoblasts: a putative explanation for why intermittent administration is needed for bone anabolism. J Biol Chem. 2003; 278:50259–50272. [PubMed: 14523023]

Chen H, Demilrap B, Schneider A, Koh A, Silve C, Wang C, McCauley LK. Parathyroid hormone and parathyroid hormone related peptide exert both pro and anti-apoptotic effects in mesenchymal cells. J Biol Chem. 2002; 277:19374–19380. [PubMed: 11897779]

Choi KY, Kim HJ, Lee MH, Kwon TG, Nah HD, Furuichi T, Toshihisa Komori Nam SH, Hyun-Jung Kim HJ, Ryoo HM. Runx-2 regulates FGF2-induced *Bmp2* expression during cranial bone development. Develop Dyn. 2005; 233:115–121.

Gospodarowicz D. Fibroblast growth factor chemical structure and biologic function. Clin Orthop Rel Res. 1990; 257:231–238.

Datta NS, Chen C, Berry JE, McCauley LK. PTHrP signalling targets cyclin D1 and induces osteoblastic cell growth arrest. J Bone Miner Res. 2005; 20:1051–1064. [PubMed: 15883646]

Datta NS, Pettway GJ, Chen C, Koh AJ, McCauley LK. Cyclin D1 is a target for the proliferative effects of PTH and PTHrP in early osteoblastic cells. J Bone Miner Res. 2007; 22:951–963. [PubMed: 17501623]

Dempster DW, Cosman F, Kurland ES, Zhou H, Nieves J, Woelfert L, Shane E, Plavetic K, Muller R, Bilezikian J, Lindsay R. Effects of daily treatment with parathyroid hormone on bone microarchitecture and turnover in patients with osteoporosis: a paired biopsy study. J Bone Miner Res. 2001; 16:1846–1905. [PubMed: 11585349]

Dong M, Guda K, Nambiar PR, Nakanishi M, Lichtler AC, Nishikawa M, Giardini C, Rosenberg DW. Azoxymethane-induced preadipocyte factor 1 (Pref-1) functions as a differentiation inhibitor in colonic epithelial cells. Carcinogenesis. 2004; 25:2239–2246. [PubMed: 15297369]

Ducy P, Zhang R, Geoffroy V, Ridall AL, Karsenty G. Osf2/cbfa1: a transcriptional activator of osteoblast differentiation. Cell. 1997:747–754. [PubMed: 9182762]

Ducy P. Cbfa1:a molecular switch in osteoblast biology. Develop. Dyn. 2000; 219:461–471.

Franceschi RT, Xiao G. Regulation of the osteoblast-specific transcription factor, Runx2: responsiveness to multiple signal transduction pathways. J Cell Biochem. 2003; 88:446–454. [PubMed: 12532321]

Friedenstein AJ, Latzinik NV, Gorskaya YuF, Luria EA, Moskvina IL. Bone marrow stromal colony formation requires stimulation by haemopoietic cells. Bone Miner. 1992; 18:199–213. [PubMed: 1392694]

Galindo M, Pratap J, Young DW, Hovhannisyan H, Im H-J, Choi J-Y, Lian JB, Stein JL, Stein GS, van Wijnen AJ. The Bone-specific Expression of Runx2 Oscillates during the Cell Cycle to Support a G1-related Antiproliferative Function in Osteoblasts. JCB. 2005; 280:20274–20285.

Globus RK, Patterson-Buckendahl P, Gospodarowicz D. Regulation of bovine bone cell proliferation by fibroblast growth factor and transforming growth factor b. Endocrinology. 1988; 123:98–105. [PubMed: 2838270]

Groth C, Lardelli M. The structure and function of vertebrate fibroblast growth factor receptor 1. Int J Dev Biol. 2002; 46:393–400. [PubMed: 12141425]

Hock JM, Gera I, Fonseca J, Raisz LG. Human parathyroid hormone (1–34) increases bone mass in ovariectomized and orchidectomized rats. Endocrinology. 1988; 122:2899–2904. [PubMed: 3371266]

Hock J, Hummer JR, Boyce R, Fonseca J, Raisz LG. Resorption is not essential for the stimulation of bone growth by hPTH(1–34) in rats in vivo. J Bone Miner Res. 1989; 4:449–458. [PubMed: 2527459]

Hock J, Krishnan V, Onyia J, Bidwell J, Stanislaus D. Osteoblast apoptosis and bone turnover. J Bone Miner Res. 2001; 16:975–984. [PubMed: 11393794]

Hodsman AB, Steer BM. Early histomorphometric changes in response to parathyroid hormone therapy in osteoporosis: evidence for *de novo* bone formation on quiescent cancellous surfaces. Bone. 1993; 14:523–527. [PubMed: 8363903]

Hodsman AB, Hanley DA, Ettinger MP, Bolognese MA, Fox J, Metcalfe AJ, Lindsay R. Efficacy and safety of human parathyroid hormone-(1–84) in increasing bone mineral density in postmenopausal osteoporosis. J Clin Endocrinol Metab. 2003; 88:5212–5220. [PubMed: 14602752]

Hurley MM, Tetradis S, Huang Y, Hock J, Kream BE, Raisz LG, Sabbieti MG. Parathyroid hormone regulates the expression of fibroblast growth factor-2 mRNA and fibroblast growth factor receptor mRNA in osteoblastic cells. J Bone Miner Res. 1999; 14:776–783. [PubMed: 10320526]

Hurley, MM.; Marie, P.; Florkiewicz, R. Fibroblast growth factor and fibroblast growth factor receptor families. In: Bilezikian, JP.; Raisz, LG.; Rodan, G., editors. Principles of bone biology. San Diego: Academic Press; 2002. p. 825-852.

Hurley M, Yao W, Lane NE. Changes in serum fibroblast growth factor 2 in patients with glucocorticoid-induced osteoporosis treated with human parathyroid hormone (1–34). 2005; 16:2080–2084.

Hurley MM, Okada Y, Xiao L, Tanaka Y, Ito M, Okimoto N, Nakamura T, Rosen CJ, Doetschaman T, Coffin JD. Impaired bone anabolic response to parathyroid hormone in Fgf2−/− and Fgf2+/− mice. Biochem Biophys Res Commun. 2006; 341:989–994. [PubMed: 16455048]

Jilka RL, Weinstein RS, Bellido T, Roberson P, Parfitt AM, Manolagos SC. Increased bone formation by prevention of osteoblast apoptosis with parathyroid hormone. J Clin Invest. 1999; 104:439–446. [PubMed: 10449436]

Jilka RL. Molecular and cellular mechanisms of the anabolic effect of intermittent PTH. Bone. 2007; 40:1434–1446. [PubMed: 17517365]

Karaplis AC, Goltzman D. PTH and PTHrP effects on the skeleton. Rev. Endocr Metab Disord. 2000; 1:331–341. [PubMed: 11706747]

Knudson C, Korsmeyer S. Bcl-2 and Bax function independently to regulate cell death. Nat Genet. 1997; 16:358–363. [PubMed: 9241272]

Komori T, Yagi H, Nomura S, Yamaguchi A, Sasaki K, Deguchi Y, Shimizu Y, Bronson RT, Gao YH, Inada M, Sato M, Okamoto R, Kitamura Y, Yoshiki S, Kishimoto T. Targeted Disruption of *Cbfa1* Results in a Complete Lack of Bone Formation owing to Maturational Arrest of Osteoblasts. Cell. 1997; 89:755–764. [PubMed: 9182763]

Kream BE, LaFrancis D, Petersen DN, Woody C, Clark S, Rowe DV, Lichtler A. Parathyroid hormone represses α1(I) collagen activity in cultured calvariae from neonatal transgenic mice. Mol Endocrinol. 1993; 7:399–408. [PubMed: 8483479]

Krishnan V, Moore TL, Ma YL, Helvering LM, Frolik CA, Valasek KM, Ducy P, Geiger AG. Parathyroid hormone bone anabolic action requires Cbfa1/Runx2-dependent signaling. Mol Endocrinol. 2003; 17:423–435. [PubMed: 12554794]

Lane NE, Thompson JM, Strewler GJ, Kinney JH. Intermittent treatment with human parathyroid hormone (hPTH[1–34]) increased trabecular bone volume but not connectivity in osteopenic rats. J Bone Miner Res. 1995; 10:1470–1477. [PubMed: 8686502]

Long F, Schipani E, Asahara H, Kronenberg H, Montminy M. The CREB family of activators is required for endochondral bone development. Development. 2001; 128:541–550. [PubMed: 11171337]

Mansukani A, Bellosta P, Sahni M, Basilico C. Signaling by fibroblast growth factors (FGF) and fiibroblast growth factor receptor-2 (FGFR2)-activating mutations block mineralization and induces apotosis in osteoblasts. J Cell Biol. 2000; 149:1297–1308. [PubMed: 10851026]

Montero A, Okada Y, Tomita M, Masato I, Tsurukami H, Nakamura T, Doetschman T, Coffin JD, Hurley MM. Disruption of the fibroblast growth factor-2 results in decreased bone mass and bone formation. J Clin Invest. 2000; 105:1085–1093. [PubMed: 10772653]

Naganawa T, Xiao L, Abogunde E, Sobue T, Kalajzic I, Sabbieti M, Agas D, Hurley MM. In vivo and in vitro comparison of the effects of FGF-2 null and haplo-insufficiency on bone formation in mice. Biochem Biophys Res Commun. 2006; 339:490–498. [PubMed: 16298332]

Neer RM, Arnaud CD, Zanchetta JR, Prince R, Gaich GA, Reginster JY, Hodsman AB, Ericksen EF, Ish-Shalom S, Genant HK, Wang O, Mitlack BH. Effects of parathyroid hormone (1.34) on fractures and bone mineral density in postmenaupausal women with osteoporosis. N. Eng. J. Med. 2001; 10:1434–1441.

Okada Y, Montero A, Zhang X, Sobue T, Lorenzo J, Doetschman T, Coffin JD, Hurley MM. Impaired osteoclast formation in bone marrow cultures of Fgf2 null mice in response to parathyroid hormone. J Biol Chem. 2003; 278:21258–21266. [PubMed: 12665515]

Otto F, Thornell AP, Crompton T, Denzel A, Gilmour KC, Rosewell IR, Stamp GW, Beddington RS, Mundlos S, Olsen DR, Selby PB, Ownen MG. Cbfa1, a candidate gene for cleidocranial dysplasia syndrome, is essential for osteoblast differentiation and bone development. Cell. 1997; 89:765–771. [PubMed: 9182764]

Pettway G, Meganck JA, Koh AJ, Keller ET, Goldstein SA, McCauley LK. Parathyroid hormone mediates bone growth through the regulation of osteoblast proliferation and differentiation. Bone. 2007; 42:806–818. [PubMed: 18234576]

Qin L, Li X, Ko JK, Partridge NC. Parathyroid hormone uses multiple mechanisms to arrest cell cycle progression of osteoblastic cells from G1 to S Phase. J Biol. Chem. 2005; 280:3104–3111. [PubMed: 15513917]

Reeve J. PTH: a future role in the management of osteoporosis? J Bone Miner Res. 1996; 11:440–445. [PubMed: 8992874]

Rodan SB, Wesolowski G, Yoon K, Rodan GA. Opposing effects of fibroblast growth factor and pertussis toxin on alkaline phosphatase, osteopontin, osteocalcin and type one collagen mRNA levels in ROS 17/2.8 cells. J Biol Chem. 1989; 264:19934–19941. [PubMed: 2479640]

Rosen CJ, Bilezikian JP. Anabolic therapy for osteoporosis. J Clin Endocrinol Metab. 2001; 86:957–964. [PubMed: 11238469]

Scutt A, Zeschnigk M, Bertram P. $PGE_2$ induces the transition from nonadherent to adherent bone marrow mesenchymal precursor cells via a cAMP/EP2-mediated mechanism. Prostaglandins. 1995; 49:383–395. [PubMed: 7480806]

Shen V, Kohler G, Huang J, Huang SS, Peck WA. An acidic fibroblast growth factor stimulates DNA synthesis, inhibits collagen and alkaline phosphatase synthesis and induces resorption in bone. Bone & Min. 1989; 7:205–219.

Swarthout JT, D'Alonzo RC, Selvamurugan N, Partridge NC. Parathyroid hormone-dependent signalling pathways regulating genes in bone cells. Gene. 2002; 282:1–17. [PubMed: 11814673]

Tan Y, Rouse J, Zhang A, Cariati S, Cohen P, Comb MJ. FGF and stress regulate CREB and ATF-1 via a pathway involving p38 MAP kinase and MAPKAP. Embo J. 1996; 15:4629–4642. [PubMed: 8887554]

Xiao G, Jiang D, Gopalakrishnan R, Franceschi RT. Fibroblast growth factor 2 induction of the osteocalcin gene requires MAPK activity and phosphorylation of the osteoblast transcription factor, Cbfa1/Runx-2. J Biol Chem. 2002; 277:36181–36187. [PubMed: 12110689]

Zhou M, Sutliff RL, Paul RJ, Lorenz JN, Hoying JB, Haundenschild CC, Moying Y, Coffin JD, Kong L, Kranias EG, Luo W, Boivin GP, Duffy JJ, Pawlowski SA, Doetschman T. Fibroblast growth factor 2 control of vascular tone. Nat Med. 1998; 4:201–207. [PubMed: 9461194]

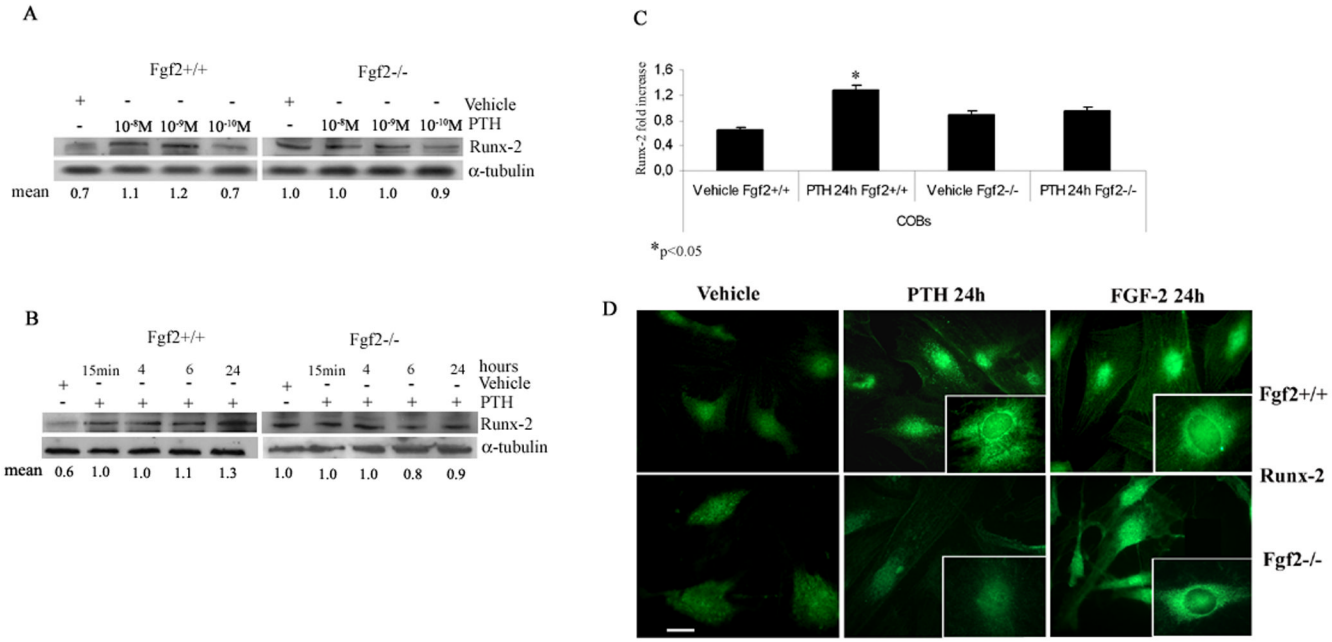


**Fig. 1. Effect of PTH on Runx-2 protein levels in COBs from Fgf2+/+ and Fgf2−/− mice**

Expression levels of Runx-2 in COBs were analyzed by Western blotting as described under methods. *A*, COBs from Fgf2+/+ and Fgf2−/− mice were treated with PTH ($10^{-8}$ M to$10^{-10}$ M) for 24 h. Proteins (5 μg) from each sample were subjected to SDS–PAGE, transferred to PVDF membrane and probed with a polyclonal anti-Runx-2 antibody. Filters were stripped and reprobed with a monoclonal anti-α-tubulin antibody to show equal amount of loading. *B*, COBs from Fgf2+/+ and Fgf2−/− were treated with PTH $10^{-9}$ M from 15 min to 24 h. Proteins (5 μg) from each sample were subjected to SDS–PAGE, transferred to PVDF membrane and probed with a polyclonal anti-Runx-2 antibody. Filters were stripped and reprobed with a monoclonal anti-α-tubulin antibody, to show equal amount of loading. *C*, Statistical analysis from a pool of four independent experiments showed that 24 h of PTH treatment increased Runx-2 protein only in Fgf2 +/+ COBs (Mean± SD. *p <0.05). *D*, Effect of PTH and FGF-2 on Runx-2 labeling pattern in COBs from Fgf2+/+ and Fgf2−/− mice. COBs from Fgf2+/+ and Fgf2−/− were treated with PTH $10^{-9}$ M or FGF-2 $10^{-9}$ M for 24h. Localization of Runx-2 was analyzed by fluorescent microscopy using a polyclonal anti-Runx-2 antibody as described under methods. Inserts clearly demonstrate the perinuclear and nuclear accumulation of Runx-2 after PTH treatment only in Fgf2+/+ COBs (green: FITC staining). Bar, 50 μm.

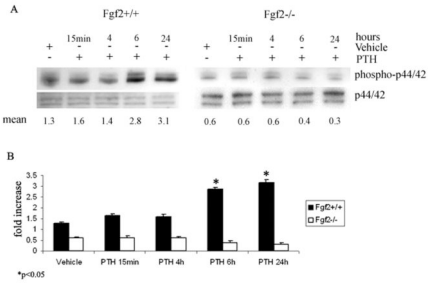


**Fig. 2. Effect of PTH on phospho-p44/42 in COBs from Fgf2+/+ and Fgf2−/− mice**

*A*, Expression levels of phospho-p44/42 in COBs were analyzed by Western blotting as described under methods. COBs from Fgf2+/+ and Fgf2−/− were treated with PTH $10^{-9}$M from 15 min to 24h. Proteins (5 μg) from each sample were subjected to SDS–PAGE, transferred to PVDF membrane and probed with a polyclonal anti-phospho-p44/42 antibody. Filters were stripped and reprobed with a polyclonal anti-p44/42 antibody to show equal loading. *B*, Statistical analysis from pool of three different experiments demonstrated that PTH increased phospho-p44/42 proteins only in Fgf2+/+ COBs. (Mean± SD *p <0.05)

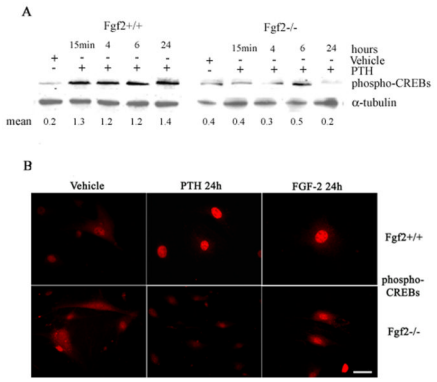


**Fig. 3. Effect of PTH on phospho-CREBs in COBs from Fgf2+/+ and Fgf2−/− mice**

*A*, Expression levels of phospho-CREBs in COBs were analyzed by Western blotting as described under methods. COBs from Fgf2+/+ and Fgf2−/− were treated with PTH $10^{-9}$ M from 15 min to 24 h. Proteins (5 μg) from each sample were subjected to SDS–PAGE, transferred to PVDF membrane and probed with a polyclonal anti-phospho-CREBs antibody. Filters were stripped and reprobed with a monoclonal anti-α-tubulin antibody to show equal amount of loading. *B*, Localization of phospho-CREBs in COBs was analyzed by fluorescent microscopy using a polyclonal anti-phospho-CREBs antibody, as described under methods (green: FITC staining). Bar, 50 μm.

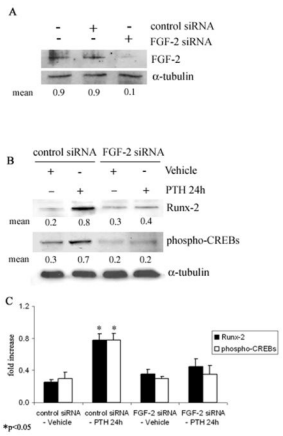


**Fig. 4. Depletion of endogenous FGF-2 expression by siRNA in COBs from Fgf2+/+ mice**

*A*, Cells were transfected with FGF-2 siRNA or control siRNA and the level of FGF-2 protein was analyzed by Western blotting as described under methods. Proteins (5 μg) from each sample were subjected to SDS–PAGE, transferred to PVDF membrane and probed with a polyclonal rabbit anti-FGF-2 antibody. Filters were stripped and reprobed with a monoclonal anti-α-tubulin antibody to show equal amount of loading. *B*, After transfection, as above described, cells were serum deprived for 24h and treated with PTH $10^{-9}$ M or vehicle from another 24 h. Proteins (5 μg) from each sample were subjected to SDS–PAGE, transferred to PVDF membrane and probed with a polyclonal anti-Runx-2 antibody or a polyclonal anti-phospho-CREBs antibody; then filters were stripped and reprobed with a monoclonal anti-α-tubulin antibody to show equal amount of loading. C, Statistical analysis from a pool of three different experiments showed that PTH increases Runx-2 and phospho-CREBs levels only in presence of FGF-2 (Mean± SD *p <0.05).

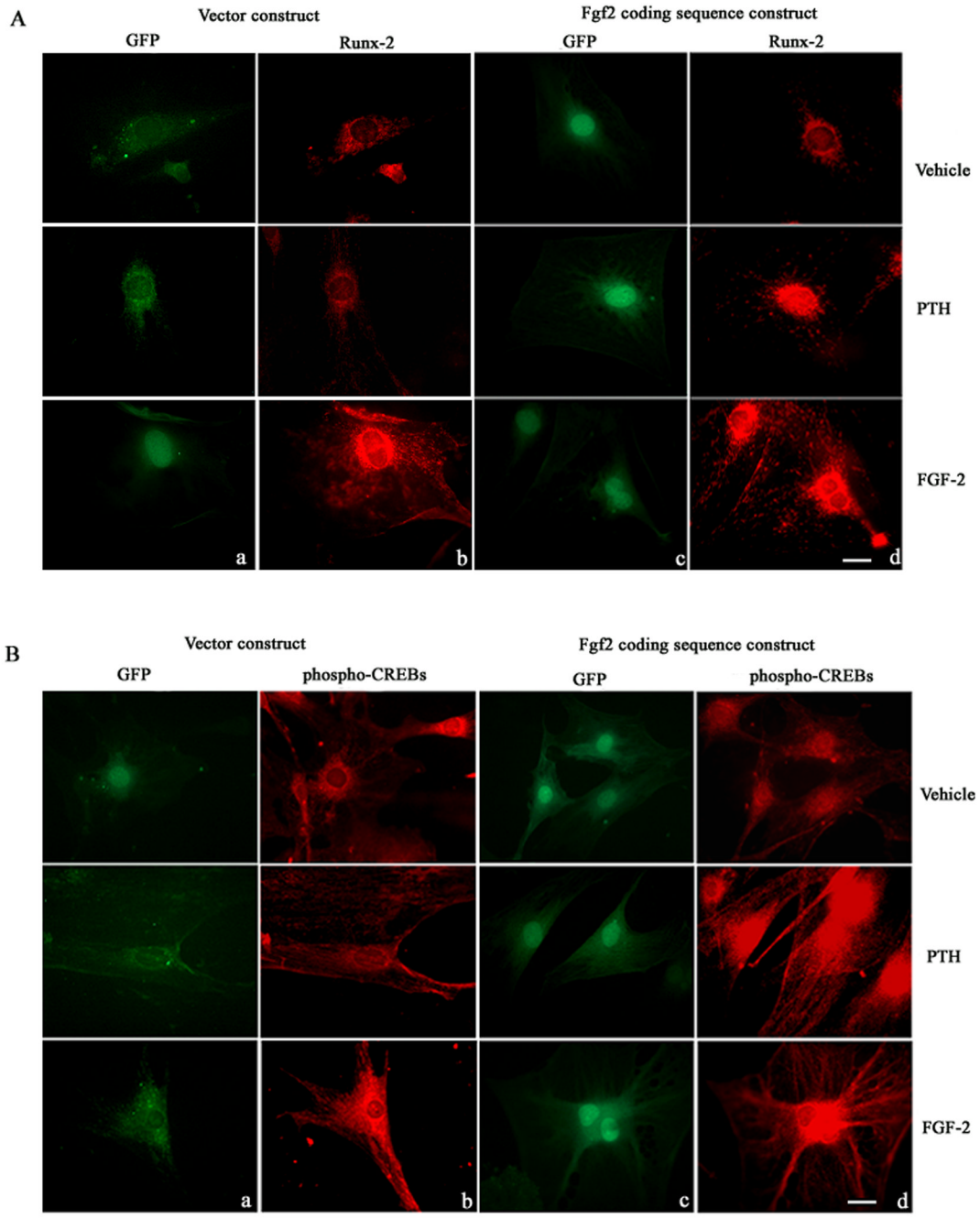


**Fig. 5. *A*, Effect of PTH and FGF-2 on Runx-2 labeling in Fgf2−/− COB cells transfected with the Fgf2 or vector construct**

COBs from Fgf2−/− mice were transfected with a FGF-2 pMg1cla construct containing the enhanced GFP (eGFP) gene used to visualize expression of protein mediated by CMV vectors. Column a: micrographs, obtained by fluorescent microscopy show GFP labelling in cells transfected with only vector construct. Column b: micrographs show labelling for Runx-2 in cells transfected with only vector construct (red: Texas Red staining). Column c: micrographs showing GFP labelling in cells transfected with Fgf2 coding sequence construct. Column d: micrographs showing labelling for Runx-2 in cells transfected with Fgf2 coding sequence construct (red:Texas Red staining). Bar, 50 μm. ***B*, Effect of PTH**

**and FGF-2 on phospho-CREB labeling in Fgf2−/− COB cells transfected with the Fgf2 or vector construct.** COBs from Fgf2−/− mice were transduced with a FGF-2 pMg1cla construct containing the enhanced GFP (eGFP) gene used to visualize expression of protein mediated by CMV vectors. Column a: micrographs, obtained by a fluorescent microscopy show GFP labeling in cells trasfected with only vector. Column b: micrographs show labelling for CREB in cells transfected with only vector (red: Texas Red staining). Column c: micrographs show GFP labeling in cells transfected with Fgf2 construct. Column d: micrographs showing labelling for phospho-CREBs in cells transfected with Fgf2 construct (red:Texas Red staining). Bar, 50 μm.

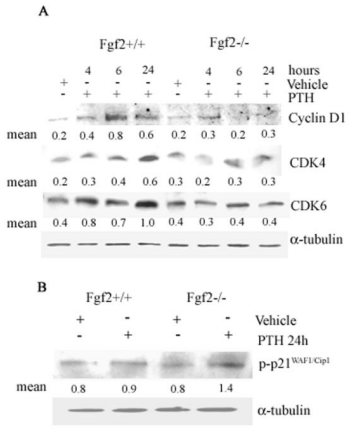


**Fig. 6. *A*, Effect of PTH on cyclin D1-cdk4/cdk6 complex in COBs from Fgf2+/+ and Fgf2−/− mice**

Expression levels of cyclin D1-cdk4/cdk6 complex were analyzed by Western blotting as described under methods. COBs from Fgf2+/+ and Fgf2−/− mice were treated with PTH $10^{-9}$ M from 4 h to 24 h. Proteins (5 μg) from each sample were subjected to SDS–PAGE, transferred to PVDF membrane and probed with polyclonal anti-cyclin D1, anti-cdk4 and anti-cdk6 antibodies. Filters were stripped and reprobed with a monoclonal anti-α-tubulin antibody to show equal amount of loading. ***B*, Effect of PTH on phospho-p21 in COBs from Fgf2+/+ and Fgf2−/− mice.** Expression levels of phospho-p21 was analyzed by Western blotting as described under methods. COBs from Fgf2+/+ and Fgf2−/− mice were treated with PTH $10^{-9}$ M for 24 h. Proteins (5 μg) from each sample were subjected to SDS–PAGE, transferred to PVDF membrane and probed with a polyclonal anti-phospho-p21 antibody. Filters were stripped and reprobed with a monoclonal anti-α-tubulin antibody to show equal amount of loading.

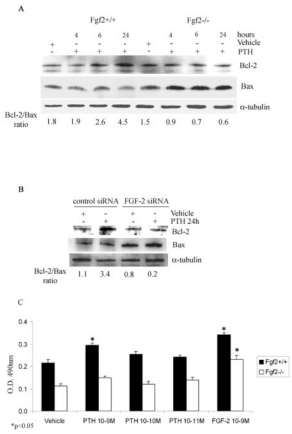


**Fig 7. Effect of PTH on Bcl-2/Bax ratio in COBs from Fgf2+/+ and Fgf2−/− mice**

Expression levels of Bcl-2 and Bax in COBs were analyzed by Western blotting as described under methods. *A*, COBs from Fgf2+/+ and Fgf2−/− were treated with vehicle or PTH $10^{-9}$ M from 4 h to 24 h. Proteins (5 μg) from each sample were subjected to SDS–PAGE, transferred to PVDF membrane and probed with a polyclonal anti-Bcl-2 antibody or with a polyclonal anti-Bax antibody. Filters were stripped and reprobed with a monoclonal anti-α-tubulin to show equal amount of loading. *B*, Cells were transfected with FGF-2 siRNA or control siRNA as described above. After transfection, cells were serum deprived for 24h and treated with PTH $10^{-9}$ M from another 24h. Proteins (5 μg) from each sample were subjected to SDS–PAGE, transferred to PVDF membrane and probed with a polyclonal anti-Bcl-2 antibody or with a polyclonal anti-Bax antibody; filters were stripped and reprobed with a monoclonal anti-α-tubulin antibody to show equal amount of loading. *C*, MTS assay. Dose-response effect of PTH on the metabolic activity of viable COBs from Fgf2+/+ and Fgf2−/− mice. Cells were 24 h serum deprived and treated with PTH, from $10^{-9}$ to $10^{-11}$ M, or vehicle for 24 h. Other cells were treated with FGF-2 ($10^{-9}$ M). Values are mean ± SEM for three different experiments. Note the significant increase of cell viability induced by PTH particularly at the concentration of $10^{-9}$ M only in Fgf2+/+ mice. *$p < 0.05$.